Electrochemical Properties of $LiNi_{0.8}Co_{0.16}Al_{0.04}O_2$ and Surface Modification with $Co_3(PO_4)_2$ as Cathode Materials for Lithium Battery

Kwang Sun Ryu,* Sang Hyo Lee,† and Yong Joon Park‡

*Department of Chemistry, University of Ulsan, Ulsan 680-749, Korea. *E-mail: ryuks@ulsan.ac.kr*
†Department of Metallurgical Engineering, Hanbat National University, Daejeon 305-719, Korea
‡Division of Advanced Industrial Engineering, Kyonggi University, Gyeonggi 443-760, Korea
Received April 2, 2008

The electrochemical and thermal stability of $LiNi_{0.8}Co_{0.16}Al_{0.04}O_2$ were studied before and after $Co_3(PO_4)_2$ coating. Different to conventional coating material such as ZrO_2 or $AlPO_4$, the coating layer was not detected clearly by TEM analysis, indicating that the $Co_3(PO_4)_2$ nanoparticles effectively reacted with surface impurities such as Li_2CO_3. The coated sample showed similar capacity at a low C rate condition. However, the rate capability was significantly improved by the coating effect. It is associated with a decrease of impedance after coating because impedance can act as a major barrier for overall cell performances in high C rate cycling. In the DSC profile of the charged sample, exothermic peaks were shifted to high temperatures and heat generation was reduced after coating, indicating the thermal reaction between electrode and electrolyte was sucessfully suppressed by $Co_3(PO_4)_2$ nanoparticle coating.

Key Words : Cathode, Lithium battery, Electrochemical properties, Surface modification

Introduction

Ni based layered oxides are interested as cathode material for lithium-ion batteries due to its higher specific capacity than commercial cathode material such as $LiCoO_2$.[1-5] The specific capacity of $LiCoO_2$ is about 160 $mAhg^{-1}$, while that of Ni-based layered oxide is 170-190 $mAhg^{-1}$. However, they do not meet the safety guidelines in the overcharged state in Li-ion cells.[6] Recently, a different approach, coating the cathode material with metal oxides nano-particles, has been reported for modifying lithium secondary batteries.[7-15] A metal oxide coating, such as TiO_2, Al_2O_3, SiO_2 and $AlPO_4$, improved capacity retention, rate capability and, in some cases, thermal stability without sacrificing the specific capacity of the cathode.

In this paper, nano-particle $Co_3(PO_4)_2$ coating was introduced for modifying one of the Ni based cathode materials, $LiNi_{0.8}Co_{0.16}Al_{0.04}O_2$. The same coating material was applied to $LiCoO_2$ in the previous report.[16] $Co_3(PO_4)_2$ nano-particles completely reacted with Li in $LiCoO_2$ resulting in the formation of a $LiCoPO_4$ phase and partially lithium deficient Li_xCoO_2. The olivine $LiCoPO_4$ phase is very electrochemically and thermally stable even after full delithiation.[17] Therefore, $Co_3(PO_4)_2$ coating is expected to improve both the electrochemical properties and thermal stability of $LiNi_{0.8}Co_{0.16}Al_{0.04}O_2$ cathode material.

Experimental

$LiNi_{0.8}Co_{0.16}Al_{0.04}O_2$ was used as a starting material and reference samples were purchased from Sumitomo Chemical. $(NH_4)_2HPO_4$ (0.45 g) and $Co(NO_3)_2 \cdot 6H_2O$ (1.5 g) were dissolved in the distilled water for the coating solution. The ammonium hydroxide was added to the solution to increase the pH to 8.5. $LiNi_{0.8}Co_{0.16}Al_{0.04}O_2$ powder (50 g) was then solowly added to the coating solution and mixed into a uniform slurry. The mixture was dried at 130 °C for five hours. The dried powder was ground and heat treated at 700 °C for five hours.

X-ray diffraction (XRD) patterns were obtained on the cathode electrode using a Philips X-ray diffractometer in the 2 θ range from 15 to 70° with monochromatized Cu-K_α radiation (λ = 1.5406 Å). Samples before and after coating were tested with scanning electron microscopy (SEM 535M, Philips) and transmission electron microscopy (CM 20 TEM, Philips, 200 kV).

For the preparation of the positive electrode, 0.15 g (3 wt.%) polyvinyl difluoride (Aldrich) was dissolved in about 12 mL of *N*-methyl-2-pyrrolidone for one hour and then 4.75 g (94 wt.%) of the sample powder and 0.15 g (3 wt.%) of Super P black (MMM Carbon Co.) were added. After a 24-hour ball mill process, the viscous slurry was coated on an aluminum foil using a surgical blade and dried at 90 °C in an oven. The obtained cathode film was hot pressed at 100 °C. The thickness of the cathode film was about 30 μm. The electrochemical cell was assembled in a dry room using the positive electrode, lithium, porous polyethylene film and 1 M $LiPF_6$ solution in a 1:1:1 weight ratio of ethylene carbonate: dimethyl carbonate: diethyl carbonate. The cells were subjected to galvanostatic cycling using a Toyo (TOSCAT 3000) charge-discharge system. Impedance measurement was carried out using a impedance/grain phase analyzer (Solartron SI 1260) in conjunction with a potentiostat (Solartron SI 1287) equipped with Z-view software, where an AC voltage of 5 mV amplitude was applied over a frequency range from 0.1 Hz to 100 kHz.

Differential scanning calorimetry (DSC) samples for the cathode were prepared by charging the cells to 4.3 V at the

slow rate of C/15. These cells were then disassembled in a dry room to remove the charged positive electrode. 4.7 mg of the positive electrode and 3 μL of fresh electrolyte were sealed in a high pressure DSC pan. The heating rate and temperature range of the DSC tests were 5 °C/min and 25-300 °C, respectively.

Results and Discussion

The phase of $LiNi_{0.8}Co_{0.16}Al_{0.04}O_2$ powder was investigated by XRD analysis, as shown in Figure 1. The XRD patterns of the coated $LiNi_{0.8}Co_{0.16}Al_{0.04}O_2$ powder are identical to those of the bare sample, even though possible formation of a nanophase on the surface because of a slight amount of coating material. Both XRD patterns can be indexed according to the $R\bar{3}m$ space group. Figure 2 shows the scanning electron microscopy (SEM) images of the bare and coated $LiNi_{0.8}Co_{0.16}Al_{0.04}O_2$ powder. The bare powders which look like big 5-8 μm sized spheres, comprise secondary small particles that are composed of smooth-edged 0.2-0.5 μm sized polyhedral primary particles. At low magnification, there was not any special difference between the coated and uncoated sample. However, a higher magnification (60000 ×) reveled that the primary particles changed into a slightly roughened surface due to a reaction with nanoparticles.

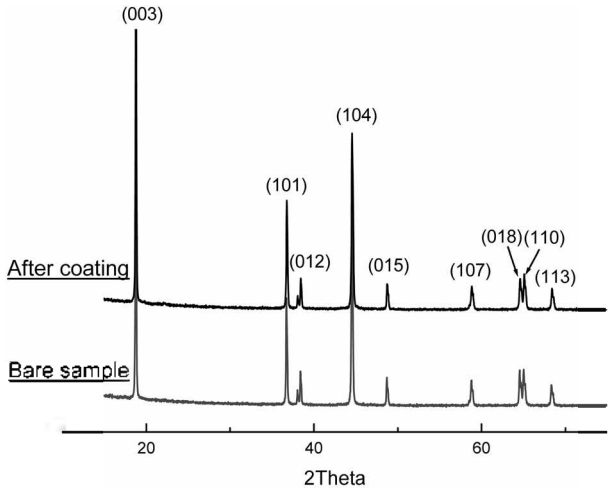

Figure 1. X-ray diffraction (XRD) patterns of $LiNi_{0.8}Co_{0.16}Al_{0.04}O_2$ powder before and after $Co_3(PO_4)_2$ coating.

A transmission electron microscopy (TEM) analysis was introduced to investigate the shape of primary particles and surface morphology in detail. Figure 3 displays the bright field of $LiNi_{0.8}Co_{0.16}Al_{0.04}O_2$ primary particles before and after coating. It is interesting that a homogeneous nanoscalar thin film layer covered the bare (uncoated) $LiNi_{0.8}Co_{0.16}Al_{0.04}O_2$ surface. In contrast, the primary particles of the coated sample could not be clearly detected as a coating layer. This finding seemed to be inconsistent with what had been observed with the earlier coated cathode material.[18-20] Most of the coated cathode material showed a distinct coating layer formed on the surface of the bare sample. According to G. V. Zhuang *et al.*, the air exposed $LiNi_{0.8}Co_{0.15}Al_{0.05}O_2$ particles were covered by an continuous layer at least 10 nm thick due to reaction between $LiNi_{0.8}Co_{0.15}Al_{0.05}O_2$ and CO_2 in the air. The formation of Li_2CO_3 is presumed to have taken place via reaction.[21]

$$LiNi_{0.8}Co_{0.15}Al_{0.05}O_2 + \frac{1}{4}x\,O_2 + \frac{1}{2}x\,CO_2 \rightarrow Li_{1-x}Ni_{0.8}Co_{0.15}Al_{0.05}O_2 + \frac{1}{2}x\,Li_2CO_3$$

Moreover, Ni-based cathode materials have rapid moisture uptakes, and Li_2CO_3 or LiOH impurities were reported to be easily formed on the surface.[22-24] Therefore, the thin film layer of bare $LiNi_{0.8}Co_{0.16}Al_{0.04}O_2$ sample observed in the TEM image must be a Li_2CO_3 and other impurity layer. The disappearance of the impurity layer after the coating treatment is likely to be due to a reaction with $Co_3(PO_4)_2$ nanoparticles. ZrO_2 and $AlPO_4$ coatings showed a clearly distinguishable coating layer form on the bulk materials because coating materials did not react with impurity phases such as Li_2CO_3 or LiOH on heat treatment temperature (700 °C)

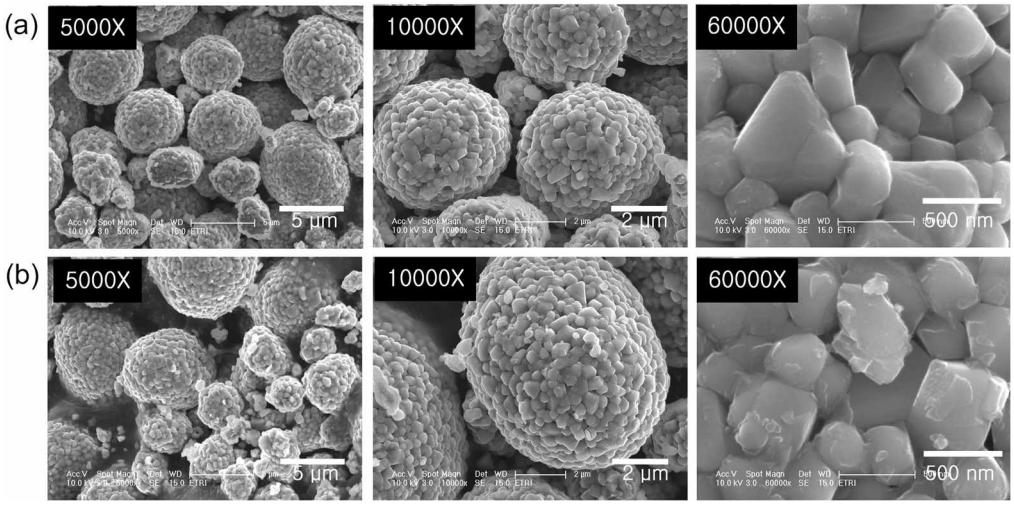

Figure 2. Scanning electron microscopy (SEM) images of $LiNi_{0.8}Co_{0.16}Al_{0.04}O_2$ powder. (a) Uncoated sample; (b) $Co_3(PO_4)_2$ coated sample.

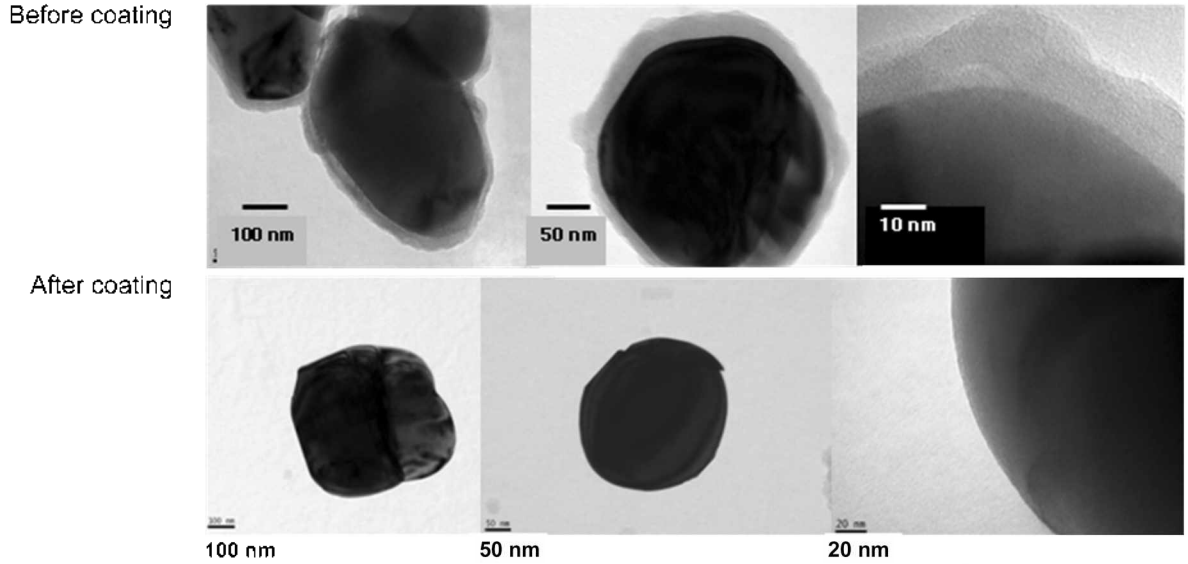

Figure 3. Bright field transmission electron microscopy (TEM) images of $LiNi_{0.8}Co_{0.16}Al_{0.04}O_2$ powder before and after $Co_3(PO_4)_2$ coating.

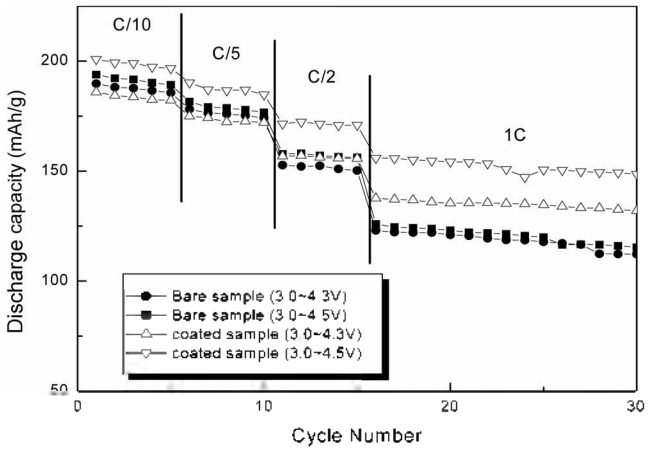

Figure 4. Discharge capacity and cyclic performances of $LiNi_{0.8}Co_{0.16}Al_{0.04}O_2$ electrode before and after $Co_3(PO_4)_2$ coating at 1/10C, 1/5C, 1/2C and 1C rate.

after the coating treatment.[9,19] As opposed to ZrO_2 or $AlPO_4$ coatings, $Co_3(PO_4)_2$ it was reported that nanoparticles were completely diffused into the surface of the cathode material and reacted with lithium of cathode material.[16] So it is likely that the Li_2CO_3 and other impurity layer on the surface of $LiNi_{0.8}Co_{0.16}Al_{0.04}O_2$ powders had compeletely reacted with $Co_3(PO_4)_2$ nanoparticles causing the distinguishable film layer to disappear. However, the surface of $LiNi_{0.8}Co_{0.16}Al_{0.04}O_2$ powders must be covered with a new phase formed by Li_2CO_3 and $Co_3(PO_4)_2$ nanoparticles. This is an expected Li_xCoPO_4 phase where there is an olivine structure.[24]

Figure 4 presents the discharge capacity and cyclic properties of the $LiNi_{0.8}Co_{0.16}Al_{0.04}O_2$ electrode before and after coating at each selected C rate. After coating, the first discharge capacity was a slight decrease in the voltage range of 3.0-4.3 V at 1/10 C rate. But it was increased a little in the voltage range of 3.0-4.5 V, in which condition the coated $LiNi_{0.8}Co_{0.16}Al_{0.04}O_2$ electrode delivered high discharge capacity of 200 $mAhg^{-1}$ in the initial cycle. With the increase of C rate, the capacity difference between the bare and the coated samples was clearly observed. At both voltage ranges, the coated sample showed superior discharge capacity to the bare sample. After 15 cycles, the coated sample delivered a remarkably higher capacity of 155 $mAhg^{-1}$ than that of the bare sample (125 $mAhg^{-1}$) in the voltage range of 3.0-4.3 V at a one C rate.

The impedance was measured to understand the improvement of rate capability of coated sample. Figure 5 presents impedance spectra for the $LiNi_{0.8}Co_{0.16}Al_{0.04}O_2$ electrode before and after coating. Generally, impedance spectra for lithium battery test cells containing cathode material exhibit two semicircles and a line inclined at a constant angle to the real axis. A semicircle located in a high frequency range is attributed to the resistance of the film that covers the surface of the cathode material; a semicircle located in a medium-to-low frequency range is related to charge transfer resistance; and an inclined line is due to Warburg impedance that is associated with lithium diffusion through the oxide electrode.[25-28] However, the impedance spectrum for bare and coated samples at a pristine state does not display two semicircles; instead, it shows a somewhat depressed one semicircle. It is likely that a semicircle related to surface film resistance was overlapped by a large semicircle associated with charge transfer resistance because the high-frequency semicircle attributable to surface film is generally smaller than the medium-to-low frequency semicircle.[29,30] The Nyquist plot of the coated sample showed a similar line profile but a much smaller semicircle than before coating in the pristine state. It was further noticed that when an electrode charged to 4.3 V or 4.5 V, the impedance reduction by coating effect become more distinct. Based on these results, it is obvious that interface resistance is reduced by the $Co_3(PO_4)_2$ coating and this effect becomes more prominent in a charged state. The impedance attributable to surface film at a high frequency range would increase after

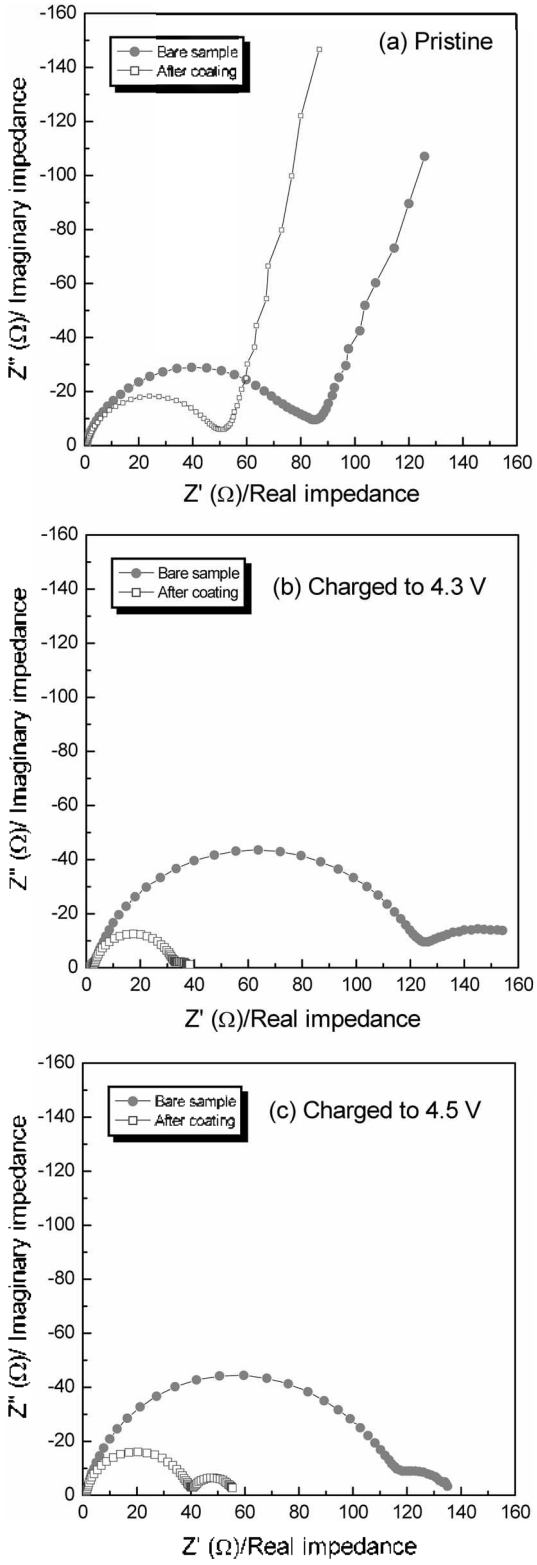

Figure 5. Nyquist plot of the cell containing $LiNi_{0.8}Co_{0.16}Al_{0.04}O_2$ electrode before and after $Co_3(PO_4)_2$ coating. (a) Pristine state; (b) Charged sample to 4.3 V; (c) Charged sample to 4.5 V.

coating treatment due to the growth of the coating thickness that hinders the permeation of electrolytes into the active material. However, it must be negligible when compared with the decrease of charge transfer resistance due to the coating effect. These results correspond well with the cell performances. Impedance may act as a major barrier for overall cell performances in high rate cycling, so lower impedance results in a better rate capability of the coated samples, as shown in Figure 4. A new small semicircle of charged sample located in a very low frequency range may associated with a new impedance factor formed by a surface reaction between electrolyte and cathode material at a high voltage range.

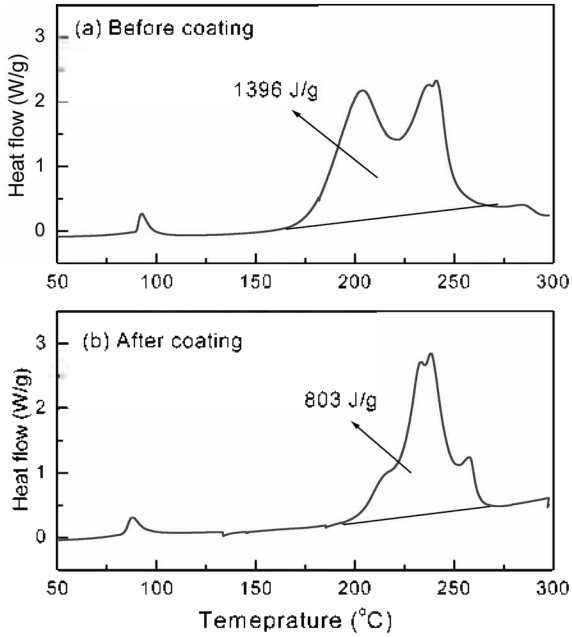

Figure 6. Differential scanning calorimetry (DSC) profile of $LiNi_{0.8}Co_{0.16}Al_{0.04}O_2$ electrode at charged state to 4.3 V. (a) Before coating; (b) After $Co_3(PO_4)_2$ coating.

Thermal stability of the $LiNi_{0.8}Co_{0.16}Al_{0.04}O_2$ electrode before and after $Co_3(PO_4)_2$ coating was investigated using DSC analysis. Thermal stability of cathode materials, especially in a charged state, is an important factor for the practical application of a lithium battery system. Figure 6 shows the DSC scan of the $LiNi_{0.8}Co_{0.16}Al_{0.04}O_2$ electrode before and after coating at the charged state to 4.3 V. The peaks below 100 °C may be related to the decomposition of organic compounds residing on the particle surface.[14,31,32] The uncoated sample started a thermal reaction with the electrolyte at around 170 °C and generated heat continuously to over 250 °C. Two large exothermic peaks produced 1396 Jg^{-1} of heat. The DSC profile of the coated sample displayed superior thermal stability to that of the uncoated sample. The onset temperature was shifted to a higher temperature of ~195 °C, and heat generation was decreased to 803 Jg^{-1}, showing that the $Co_3(PO_4)_2$ coating effectively retards the reaction between electrode and electrolyte in a charged state and enhances thermal stability of the electrode.

Conclusions

The electrochemical and thermal stability of the $LiNi_{0.8}$-

$Co_{0.16}Al_{0.04}O_2$ electrode was examined before and after $Co_3(PO_4)_2$ coating. The air exposed $LiNi_{0.8}Co_{0.16}Al_{0.04}O_2$ particles were covered by a continuous Li_2CO_3 and impurity layer at least 10 nm thick due to a reaction between $LiNi_{0.8}Co_{0.16}Al_{0.04}O_2$ and CO_2 in the air. After coating, the impurity layer disappeared because the $Co_3(PO_4)_2$ reacted with it during heat treatment. The $LiNi_{0.8}Co_{0.16}Al_{0.04}O_2$ particles may be covered with new coating film formed by an impurity phase and $Co_3(PO_4)_2$ nanoparticles although the coating film was not clearly observed by a TEM image due to the high reactivity of $Co_3(PO_4)_2$ nanoparticles. The formation of a new coating film on the surface of $LiNi_{0.8}Co_{0.16}Al_{0.04}O_2$ particles reduced interface resistance and enhanced rate capability of the $LiNi_{0.8}Co_{0.16}Al_{0.04}O_2$ electrode. Moreover, it effectively suppressd the reaction between electrode and electrolyte in a charged state and improved the thermal stability of the electrode.

Acknowledgments. This work was supported by the Division of Advanced Batteries in NGE Program (Project No. 10016454).

References

1. Li, W.; Reimers, J. N.; Dahn, J. R. *Solid State Ionics* **1993**, *67*, 123.
2. Nishida, Y.; Nakane, K.; Satoh, T. *J. Power Sources* **1997**, *68*, 561.
3. Omanda, H.; Brousse, T.; Marhic, C.; Schleich, D. M. *J. Electrochem. Soc.* **2004**, *151*, A922.
4. Belharouak, I.; Lu, W.; Vissers, D.; Amine, K. *Electrochem. Commu.* **2006**, *8*, 329.
5. Shaju, K. M.; Subba Rao, G. V.; Chowdari, B. V. R. *J. Electrochem. Soc.* **2004**, *151*, A1324.
6. Takami, N.; Inagaki, H.; Ueno, R.; Kanda, M. *Paper presented at the 11th International Meeting on Lithium Batteries*; Monterey, CA, June, 2002; pp 23-28.
7. Cho, J.; Kim, Y. J.; Kim, T.-J.; Park, B. *Angew. Chem., Int. Ed. Engl.* **2001**, *40*, 3367.
8. Cho, J.; Kim, Y. J.; Park, B. *Chem. Mater.* **2000**, *12*, 3788.
9. Cho, J.; Lee, J.-G.; Kim, B.; Park, B. *Chem. Mater.* **2003**, *15*, 3190.
10. Cho, J.; Kim, Y. J.; Park, B. *J. Electrochem. Soc.* **2001**, *148*, A1110.
11. Zhang, Z. R.; Liu, H. S.; Gong, Z. L.; Yang, Y. *J. Electrochem. Soc.* **2004**, *151*, A599.
12. Cho, J. *Electrochem. Commu.* **2003**, *5*, 146.
13. Kim, Y. J.; Kim, H.; Kim, B.; Ahn, D.; Lee, J.-G.; Kim, T.-J.; Son, D.; Cho, J.; Kim, Y.-W.; Park, B. *Chem. Mater.* **2003**, *15*, 1505.
14. Cho, B.; Kim, H.; Park, B. *J. Electrochem. Soc.* **2004**, *151*, A1707.
15. Amine, K.; Yasuda, H.; Yamachi, M. *Electrochem. Solid State Lett.* **2000**, *3*, 178.
16. Lee, H.; Kim, M. G.; Cho, J. *Electrochem. Commu.* **2007**, *9*, 149.
17. *Nanostructures and Nanomaterials*; Gao G., Ed.; World Science Publishing Co. Ltd.: Singapore, 2004.
18. Chen, Z.; Dahn, J. R. *Electrochem. Solid State Lett.* **2002**, *5*, A213.
19. Cho, J.; Kim, Y. J.; Kim, B.; Lee, J.-G.; Park, B. *Angew. Chem., Int. Ed. Engl.* **2003**, *42*, 1618.
20. Cho, J.; Lee, J.-G.; Kim, B.; Kim, T.-G.; Kim, J.; Park, B. *Electrochimica Acta* **2005**, *50*, 4182.
21. Zhuang, G. V.; Chen, G.; Shim, J.; Song, X.; Ross, P. N.; Richardson, T. J. *J. Power Sources* **2004**, *134*, 293.
22. Liu, H. S.; Zhang, Z. R.; Gong, Z. L.; Yang, Y. *Electrochem. Solid State Lett.* **2004**, *7*, A190.
23. Matsumoto, K.; Kuzuo, R.; Takeya, K.; Yamanaka, A. *J. Power Sources* **1999**, *81-82*, 558.
24. Kim, Y.; Cho, J. *J. Electrochem. Soc.*, accepted.
25. Park, Y. J.; Ryu, K. S.; Park, N.-G.; Hong, Y.-S.; Chang, S. H. *J. Electrochem. Soc.* **2002**, *149*(5), A597.
26. Bao, S.-J.; Liang, Y.-Y.; Zhou, W.-J.; He, B.-L.; Li, H.-L. *J. Power Sources* **2006**, *154*, 239.
27. Aurbach, D.; Markovsky, B.; Rodkin, A.; Levi, E.; Cohen, Y. S.; Kim, H.-J.; Schmidt, M. *Electrochimica Acta* **2002**, *47*, 4291.
28. Barsoukov, E.; Kim, D. H.; Lee, H.-S.; Lee, H.; Yakovleva, M.; Gao, Y.; Engel, J. F. *Solid State Ionics* **2003**, *161*, 19.
29. Thomas, M. G. S. R.; Bruce, P. G.; Goodenough, J. B. *J. Electrochem. Soc.* **1985**, *132*, 1521.
30. Vetter, J.; Novak, P.; Wagner, M. R.; Veit, C.; Moller, K.-C.; Besenhard, J. O.; Winter, M.; Wohlfahrt-Mehrens, M.; Vogler, C.; Hammouche, A. *J. Power Sources* **2005**, *147*, 269.
31. Andersson, A. M.; Abraham, D. P.; Haasch, R.; MacLaren, S.; Liu, J.; Amine, K. *J. Electrochem. Soc.* **2002**, *149*, A1358.
32. Yamaki, J.-I.; Takatsuji, H.; Kawamura, T.; Egashira, M. *Solid State Ionics* **2002**, *148*, 241.